

Magnetic Ionic Liquids

A Magnetic Ionic Liquid Based on Tetrachloroferrate Exhibits Three-Dimensional Magnetic Ordering: A Combined Experimental and Theoretical Study of the Magnetic Interaction Mechanism

Abel García-Saiz,^[a] Pedro Migowski,^[b] Oriol Vallcorba,^[c] Javier Junquera,^[a] Jesús Angel Blanco,^[d] Jesús Antonio González,^[a] María Teresa Fernández-Díaz,^[e] Jordi Rius,^[c] Jairton Dupont,^[b] Jesús Rodríguez Fernández,^[a] and Imanol de Pedro^{*[a]}

Abstract: A new magnetic ionic liquid (MIL) with 3D anti-ferromagnetic ordering has been synthetized and characterized. The information obtained from magnetic characterization was supplemented by analysis of DFT calculations and the magneto-structural correlations. The result gives no evidence for direct iron-iron interactions, corroborating that the 3D magnetic ordering in MILs takes place via super-exchange coupling containing two diamagnetic atoms intermediaries.

Responsive materials for which chemical or physical properties can be tuned by applying an external stimulus are appealing in view of their potential applications.^[1] New sources of such materials could be the magnetic ionic liquids (MILs), the physicochemical properties (viscosity, melting point, chemical stability, high ion conductivity, etc.) of which can be controlled by external magnetic fields.^[2] Typically, MILs are composed of a metal-containing anion (such as iron, cobalt, manganese, copper and so forth) and an organic cation, generally imidazolium, pyrrolidinium, pyridinium or tetraalkylphosphonium.^[3,4] Nowadays, the development of these MILs has made possible the combination of different rare-earth ions (neodymium, gadolinium, dysprosium),^[5] chiral amionacids (MCILs),^[6] bimagnet-

ic ions^[7] or heteroanions.^[8] Therefore, the synthesis, study and application,^[9,10] of these smart materials are increasing exponentially, and it is necessary to provide a complete picture of the crystal structure and the main magnetic interactions in play.

During the last few years, most efforts have focused upon understanding the intermolecular interactions within ILs,^[11] including Coulomb, dipole–dipole, van der Waals, dispersion and hydrogen-bond interactions.^[12] From a magnetic point of view, the reported crystal structures of most MILs show no magnetic coupling between the paramagnetic metal centres,^[3,9,13] since the distances between metal ions are too large (more than 6 Å) to allow significant long-range magnetic interactions. Thus, it was generally assumed that magnetic interactions were negligible in MILs and so they were not expected to exhibit three-dimensional (3D) magnetic ordering. However, the situation changed drastically after the experimental confirmation of a 3D ordering below 4 K^[14] in the 1-ethyl-3-methylimidazolium tetrachloroferrate, Emim[FeCl₄]⁻, and its pressure-induced magnetic transition from antiferromagnetic to ferrimagnetic behaviour.^[15] We now address the challenge of understanding the magnetic interactions of MILs with a comprehensive combination of experimental and first-principle-based theoretical methods to unravel the connection between the crystal structure and the magnetic interaction mechanism in a new MIL: 1,3-dimethylimidazolium tetrachloroferrate, Dimim[FeCl₄]⁻. We point to the electron-transfer transitions due to a partial covalent bond between the Fe and Cl atoms in [FeCl₄]⁻ complexes as the driving force for the mechanism of the magnetic interaction in MILs based on tetrachloroferrate exhibiting three-dimensional ordering.

The thermal properties of Dimim[FeCl₄]⁻ were examined by differential scanning calorimetry (DSC), thermogravimetric analysis (TGA) and heat capacity measurements (Figure S1 to S3 in the Supporting Information, including extra information on the thermal investigations). Two solid–solid (s–s) phase transitions around 332 and 285 K are observed upon cooling from above the melting point (364 K) down to 2 K, in good agreement with other MILs based on imidazolium ions, which indicate several solid–solid transitions detected by thermal analysis.^[16] The highest temperature solid phase was labelled phase **III** and the other two phases **II** and **I**, respectively (lowest temperature). The TGA experiment indicates that Dimim[FeCl₄]⁻ starts to decompose at about 624 K.

[a] A. García-Saiz, Prof. J. Junquera, Prof. J. A. González, Prof. J. Rodríguez Fernández, Dr. I. de Pedro
Facultad de Ciencias, Universidad de Cantabria
Cantabria Campus Internacional, 39005 Santander (Spain)
Fax: (+34) 942-201402
E-mail: depedrov@unican.es

[b] Dr. P. Migowski, Prof. J. Dupont
Universidade Federal do Rio Grande do Sul
Porto Alegre—Rio Grande do Sul, 90040-060 (Brazil)

[c] Dr. O. Vallcorba, Prof. J. Rius
Institut de Ciència de Materials de Barcelona (CSIC)
Campus de la UAB, 08193 Bellaterra, Catalunya (Spain)

[d] Prof. J. A. Blanco
Departamento de Física
Universidad de Oviedo, 33007 Oviedo (Spain)

[e] Dr. M. T. Fernández-Díaz
Institut Laue-Langevin, BP 156X
38042 Grenoble Cedex (France)

 Supporting information for this article is available on the WWW under <http://dx.doi.org/10.1002/chem.201303602>.

The crystal structures of phase **II** and phase **I**, listed in the Supporting Information and CIF files, were resolved from neutron diffraction patterns recorded at room temperature (RT) and 9 K, respectively. Due to the high quality of the data even the hydrogen atoms could be located during the Rietveld refinement. Phase **II** is stable at RT and crystallizes in the non-centrosymmetric monoclinic space group $P2_1$ (No. 4) [$a=6.542(3)$, $b=14.037(3)$, $c=6.536(3)$ Å, $\beta=90.01(3)^\circ$, $V=600.2(4)$ Å 3 , $Z=2$, $\rho_{\text{calcd}}=1.631$ g cm $^{-3}$, $T=300$ K]. Phase **I** crystallizes in the non-centrosymmetric orthorhombic space group $P2_12_12_1$ (No. 19) [$a=9.092(1)$, $b=13.731(2)$, $c=8.974(1)$ Å, $V=1120.2(3)$ Å 3 , $Z=4$, $\rho_{\text{calcd}}=1.748$ g cm $^{-3}$, $T=9$ K]. Both structures can be described as layers of cations and anions stacked along the b axis, with the closest Fe–Fe distances being more than 6 Å inside a layer. The presence of a 2_1 screw axis in both phases yields a change in the orientation of the [FeCl $_4$] $^-$ metal complex anions from layer to layer (see inset of Figure 1 and

well as the cation and anion orientation. Each [FeCl $_4$] $^-$ tetrahedron is stacked with six Cl–Cl contacts (<3.9 Å); two in a one-dimensional zigzag manner along the b axis (with slightly longer distances, 3.87(3) Å) and four in two linear chains propagated along the bisectors of the ac plane (3.63(4) (2×), 3.81(4) Å (2×)). No π -d interactions of the aromatic rings with the [FeCl $_4$] $^-$ metal complexes are observed in either phase, because the distances between them (near 4 Å) are considerably larger than the sum of the van der Waals (vdw) radii of C(H) and Cl atoms (3.57 Å).^[18] The Dimim cation displays six and twelve weak (long) hydrogen bonds^[19] for phases **II** and **I**, respectively, according to the IUPAC rule^[20] (Figure S7 and Table S5 in the Supporting Information). It should be mentioned that the typical most acidic hydrogen atom of the imidazolium ring, C2–H position,^[21] is not involved in the hydrogen bond network of phase **II** (nomenclature depicted in Figure S7 in the Supporting Information). Although this issue differs from the data reported for the Emim $_2$ [MCl $_4$] ($M=\text{Co, Ni}$ and Fe)^[17] and DimimCl (Dimim=1,3-dimethylimidazolium) ionic liquids,^[22] in which the strongest hydrogen bond was located in this position; similar behaviour was observed in the Emim[BF $_4$]^[23] and Emim[FeCl $_4$]^[16a] MILs. In phase **I**, significantly stronger (shorter) hydrogen bonds are found, which is consistent with the Raman spectra.^[24] At 4 K, the Raman bands of the C–H stretching modes of the imidazolium ring, located between 3100 and 3200 cm $^{-1}$, increase in intensity, which is characteristic for strong hydrogen bonds at the C2 and C4/5 positions.^[19] In addition, in the low-frequency range, a splitting of the Raman modes of the [FeCl $_4$] $^-$ complex, associated to the crystallographic phase transition, was detected (Figure S8 of the Supporting Information).

Measurements of magnetic susceptibility as a function of temperature show a sharp maximum at approximately 5.6 K (Figure 1), indicating the existence of a 3D antiferromagnetic ordering. This result indicates that a smaller chain length in the imidazolium cation [from Bmin $^+$ that shows no 3D ordering through Emim $^+$ (4 K) to Dimim $^+$ (5.6 K)] stabilizes the magnetic ordering. Above 10 K, a paramagnetic behaviour is displayed, with a $\chi_m T$ value of 4.25 emuKmol $^{-1}$ Oe $^{-1}$ (5.83 μ_B) at room temperature. At temperatures higher than 10 K, the magnetic susceptibility data follow the Curie–Weiss law with Weiss temperatures, θ_p , close to –7.0 K with a Curie constant of $C=4.34$ emuKmol $^{-1}$ Oe $^{-1}$ [see Eq. (1) in Supporting Information]. This value corresponds to an effective paramagnetic moment (μ_{eff}) of 5.88 μ_B per Fe ion; this agrees with the expected value of 4.375 emuKmol $^{-1}$ Oe $^{-1}$ (5.92 μ_B) for an Fe $^{3+}$ ion with a magnetic spin $S=5/2$.^[25] Due to the anisotropy of the crystal, a combination of a modified expression of the one-dimensional Bonner and Fisher model,^[26] for the interplane interactions, and a two-dimensional Rushbrook and Wood model,^[27] for the intraplane interactions, was used to extract the magnetic exchange couplings between the Fe $^{3+}$ ions (see magnetic fitting calculations in the Supporting Information). The best fit leads to the parameters $J_\perp=-0.511$ K for the interplane exchange interaction and $J_{||}=-0.359$ K value for the intraplane interactions with $g=2.03$. These small values point to a very weak antiferromagnetic interactions, in accordance with the large dis-

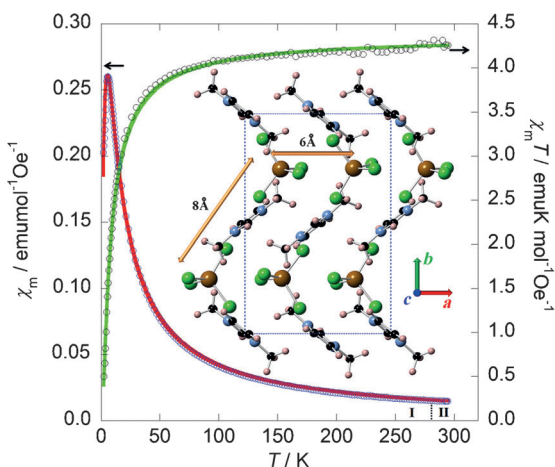


Figure 1. Temperature dependence of χ_m (blue circles) and $\chi_m T$ (black circles) for Dimim[FeCl $_4$] measured under 1 kOe. The solid red and green lines are the fit according to Equation (2) in the Supporting Information. The inset shows the crystal structure view along the [001] direction of phase **I** at 9 K. Brown (iron), green (chloride), black (carbon), blue (nitrogen) and light pink (hydrogen). The dotted square represents the unit cell.

Figure S6 in the Supporting Information). This tetrahedrally coordinated anion is fairly regular (mean values of Cl–Fe–Cl bond angles are 109(2) $^\circ$ for **I** and 110(3) $^\circ$ for **II**) with slightly different bond lengths for phase **I** and **II** (respective mean values 2.16(2) and 2.19(3) Å). The Dimim cations lie antiparallel to each other along the b direction, and are stacked nearly identically one above the other in the a and c directions, although slightly distorted in **I**. The dihedral angles of the methyl groups to the imidazolium ring [$\measuredangle(\text{C}-\text{N}-\text{C}-\text{N})$] in both phases range from 177 to 179 $^\circ$. The refined values for the C–C and C–N bond lengths lie in the expected range and are comparable to those found in other imidazolium compounds, for example, in Bmim $_2$ [XCl $_4$] (Bmim=1-butyl-3-methylimidazolium X=Fe, Ni and Co)^[17] and Emim[FeCl $_4$].^[16a]

The topologies of the unit cell in both phases are quite similar, showing virtually the same cation–anion arrangement as

tances between the iron-complex anions and the literature values for this type of magnetic pathway.^[28]

Neutron powder diffraction experiments at temperatures lower than 10 K show that the $P_{2}2_12_1$ symmetry of phase I is maintained below the ordering temperature, with small shifts in the Bragg reflections associated with lattice contraction. Difference patterns resulting from subtracting the nuclear contribution (pattern at 9 K) from the nuclear and magnetic ones, reveal, below 6 K, a sharp Bragg peak superimposed on a very broad diffuse background (see Figure S11 of the Supporting Information). This additional elastic intensity at low temperature confirms the onset of a magnetic ordering ($T_N=5.5$ K). If we consider that the magnetic moment of Fe^{+3} ($S=5/2$) is partially delocalized in the chloride ion (see below), the intensities of the magnetic peaks obtained should be very weak, but sufficient to allow 3D antiferromagnetic ordering to be observed. The presence of diffuse scattering could be the signature of additional short-range magnetic ordering superposed to the 3D ordering, which increases in a monotonous way below T_N , as observed in other geometrically frustrated antiferromagnetic materials.^[29]

Below 5 K the magnetic interactions became cooperative despite the very long (6–8.5 Å) superexchange pathway. For that reason knowledge of the spin-density distribution is of crucial importance to the understanding the magnetic interaction mechanism in Dimim[FeCl_4]. From the atomic structure the most likely exchange pathways should be of the Fe–Cl–Cl–Fe type (Figure 2). The electron-transfer transitions due to a partial covalent bonding produce a spin delocalization^[30] that would strengthen the interactions between magnetic orbitals localized in different tetrachloride ferrate units.^[31] In order to substantiate this claim, density functional theory (DFT) calculations were carried out within the new formalism to deal with van der Waals interactions,^[11c,32] which have been successfully applied to the study of ILs.^[33] Different magnetic configurations have been tried, with the G-type antiferromagnetic phase being the most stable one (see detail of DFT analysis in the Supporting Information). Figure 2 also shows the spin density of the interplane exchange magnetic interaction for the most stable phase on the *ab* plane, which contains two Fe and two Cl atoms. The different sign in the spin density in neighbouring [FeCl₄][−] tetrahedron along the *b* axis is an indication of the antiferromagnetic configuration. As can be seen, the spin density is not strictly localized on the iron ions, but is partially delocalized onto the first chloride neighbours. The sum of the Mulliken populations of the iron and the four neighbouring chloride atoms is equal to 4.98(1) μ_B . This agrees with the expected spin distribution of Fe^{+3} ion with a magnetic spin $S=5/2$ (5 μ_B). The quantity of spin transferred from the Fe^{+3} ion toward its neighbours ranges from 0.27 to 0.25 μ_B (The sum of the spin transferred per Fe^{+3} is 1.06 μ_B ; 21% of the expected saturation value of 5 μ_B .) Similar results are obtained by integrating the spin-polarized charge density in non-overlapping spheres centred on the different atoms. These reflect a stronger covalence of the Fe–Cl bond compared to other metal–Cl bonds (M=Ni, Cu and Co),^[34] but they are in good agreement with those detected in other Fe^{+3} compounds (for $\text{K}_2\text{FeCl}_5\cdot\text{H}_2\text{O}$

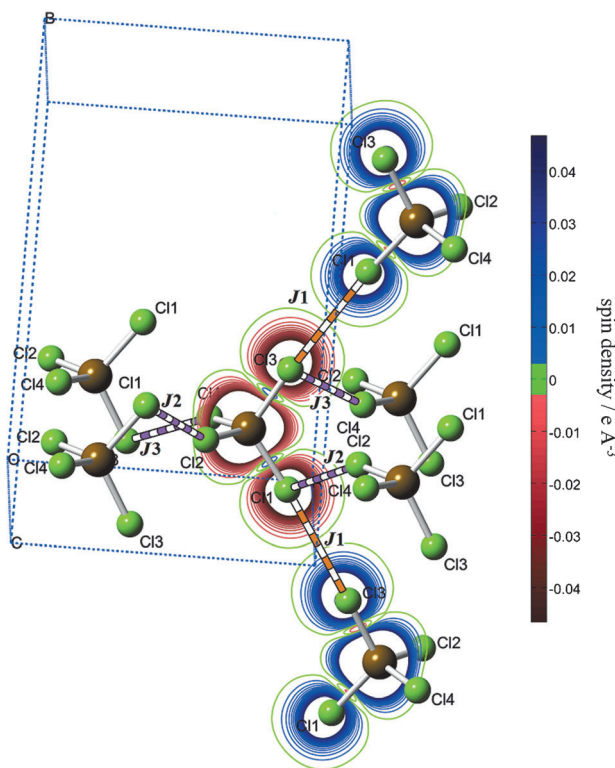


Figure 2. Schematic view of the possible exchange pathways for Dimim-[FeCl₄], through Fe–Cl–Cl–Fe bridges, are shown. The picture also displays the projection of the induced spin density onto the Fe_2L_2 plane ($z/c=0.26$) for the interplane exchange magnetic interaction at 0 K. The levels are (0.05 e Å³) with steps of 0.005 e Å³. Only the low-density levels are drawn.

and $\text{Rb}_2\text{FeBr}_5\cdot\text{H}_2\text{O}$, 17 and 21% spin delocalization, respectively).^[28b]

DFT calculations have also been successfully applied to the estimation of the exchange coupling constants, J , for a variety of transition-metal complexes.^[35] From the difference in energy between the magnetic configurations, the value of the exchange magnetic couplings was inferred, arriving at the same qualitative results as before: weak antiferromagnetic coupling and stronger interaction between planes.

The analysis of the magnetostructural correlations in Dimim-[FeCl₄] will contribute to elucidating one important open question: the reason why interplane magnetic interactions are stronger than intraplane ones. Although the Cl–Cl distances obtained are slightly longer than the sum of the van der Waals radii of two Cl atoms (3.60 Å), the data show a remarkable agreement with the contact distances reported in other metal–organic materials^[18] that show this type of magnetic coupling. In the crystal structure of I, all the [FeCl₄][−] metal complexes are stacked upon one another in a three-dimensional manner with several Cl–Cl contacts (see Figure 2, and Figure S12 and Table S10 of Supporting Information). In this sense, it is possible to define a J interplane coupling (J_{\perp} or J_1), which gives rise to zig-zag chains propagating along the *b* direction with two Fe–Cl–Cl–Fe connections, the angles of which range from 173.2 to 174.7°. This magnetic coupling leads to antiferromagnetic interactions. In addition to J_1 , there are two intraplane interac-

tions J_{\parallel} (J_2 and J_3), which connect the iron atoms in zig-zag chains in the *ac* plane, with similar Fe–Fe distances. For these intraplane interactions, the antiferromagnetic couplings observed imply an unusual combination of exchange angles: 1) Fe–Cl–Cl, which varies between 87.0 and 93.3° and 2) Cl–Cl–Fe, which ranges from 154.4 to 158.2°. If one assumes that the magnetic exchange through the double halide bridges depends on both 1) the degree of delocalization of spin density from the metal ion to the halide, and 2) the orbital overlap between the two non-bonding halide ions,^[36] J_{\perp} should have a higher value (antiferromagnetic coupling near to 180° in both angles) than J_{\parallel} . These results confirm those obtained by the magnetic susceptibility fitting and DFT calculations.

In summary, a novel magnetic ionic liquid (MIL) with 3D antiferromagnetic ordering has been synthesized and characterized. The information obtained from magnetic characterization was supplemented by analysis of DFT calculations and the magnetostructural correlations. The result gives no evidence for direct iron–iron interactions, corroborating that the 3D magnetic ordering in MILs takes place through superexchange coupling via two diamagnetic intermediaries. The DFT calculations reflect the fact that the spin density of the iron ions is spread over the chloride atoms, showing a higher superexchange magnetic interaction between the planes.

Experimental Section

Details of the synthesis and characterisation of the MIL can be found in the Supporting Information. CCDC-973942 (phase I) and 973943 (phase II) contain the supplementary crystallographic data for this paper. These data can be obtained free of charge from The Cambridge Crystallographic Data Centre via www.ccdc.cam.ac.uk/data_request/cif.

Acknowledgements

Financial support from the Spanish Ministerio de Ciencia e Innovación (Project MAT2011-27573-C04) is acknowledged. This work has been carried out within the framework of the MALTA Consolider Ingenio 2010 (Ref. CSD2007-00045). The authors thankfully acknowledge the computer resources, technical expertise and assistance provided by the Red Española de Supercomputación. We also acknowledge Jorge Kohanoff and Pablo García for their guidance and support with regard to the theoretical calculations and Becas Iberoaméricas Jóvenes Profesores Investigadores 2011, Santander Universidades.

Keywords: density functional calculations • ionic liquids • magnetic properties • structure elucidation

- [1] E. Coronado, G. Minguez Espallargas, *Chem. Soc. Rev.* **2013**, *42*, 1525–1539.
- [2] T. Torimoto, T. Tsuda, K.-i. Okazaki, S. Kuwabata, *Adv. Mater.* **2010**, *22*, 1196–1221.
- [3] R. E. Del Sesto, T. M. McCleskey, A. K. Burrell, G. A. Baker, J. D. Thompson, B. L. Scott, J. S. Wilkes, P. Williams, *Chem. Commun.* **2008**, *0*, 447–449.

- [4] T. Peppel, M. Köckerling, M. Geppert-Rybczyńska, R. V. Ralys, J. K. Lehmann, S. P. Verevkin, A. Heintz, *Angew. Chem.* **2010**, *122*, 7270–7274; *Angew. Chem. Int. Ed.* **2010**, *49*, 7116–7119.
- [5] B. Mallick, B. Balke, C. Felser, A.-V. Mudring, *Angew. Chem.* **2008**, *120*, 7747–7750; *Angew. Chem. Int. Ed.* **2008**, *47*, 7635–7638.
- [6] K. Tanaka, F. Ishiguro, Y. Chujo, *J. Am. Chem. Soc.* **2010**, *132*, 17649–17651.
- [7] C.-X. Miao, J.-Q. Wang, B. Yu, W.-G. Cheng, J. Sun, S. Chanfreau, L.-N. He, S.-J. Zhang, *Chem. Commun.* **2011**, *47*, 2697–2699.
- [8] P. Brown, C. P. Butts, J. Eastoe, E. Padron Hernandez, F. L. d. A. Machado, R. J. de Oliveira, *Chem. Commun.* **2013**, *49*, 2765–2767.
- [9] Y. Funasako, T. Mochida, T. Inagaki, T. Sakurai, H. Ohta, K. Furukawa, T. Nakamura, *Chem. Commun.* **2011**, *47*, 4475–4477.
- [10] P. Brown, A. Bushmelev, C. P. Butts, J. Cheng, J. Eastoe, I. Grillo, R. K. Heenan, A. M. Schmidt, *Angew. Chem.* **2012**, *124*, 2464–2466; *Angew. Chem. Int. Ed.* **2012**, *51*, 2414–2416.
- [11] a) K. Binnemans, *Chem. Rev.* **2007**, *107*, 2592–2614; b) I. J. B. Lin, C. S. Vasam, *J. Organomet. Chem.* **2005**, *690*, 3498–3512; c) J. Dupont, *Acc. Chem. Res.* **2011**, *44*, 1223–1231.
- [12] a) H. Weingärtner, *Angew. Chem.* **2008**, *120*, 664–682; *Angew. Chem. Int. Ed.* **2008**, *47*, 654–670; b) J. Dupont, *J. Braz. Chem. Soc.* **2004**, *15*, 341–350.
- [13] H. Mehdi, K. Binnemans, K. Van Hecke, L. Van Meervelt, P. Nockemann, *Chem. Commun.* **2010**, *46*, 234–236.
- [14] a) Y. Yoshida, G. Saito, *J. Mater. Chem.* **2006**, *16*, 1254–1262; b) I. de Pedro, D. P. Rojas, J. Albo, P. Luis, A. Irabien, J. A. Blanco, J. Rodriguez Fernandez, *J. Phys. Condens. Matter* **2010**, *22*, 296006; c) I. de Pedro, D. P. Rojas, J. A. Blanco, J. Rodriguez Fernandez, *J. Magn. Magn. Mater.* **2011**, *323*, 1254–1257.
- [15] A. García-Saiz, I. de Pedro, J. A. Blanco, J. González, J. R. Fernández, *J. Phys. Chem. B* **2013**, *117*, 3198–3206.
- [16] a) T. Bäcker, O. Breunig, M. Valldor, K. Merz, V. Vasylyeva, A.-V. Mudring, *Cryst. Growth Des.* **2011**, *11*, 2564–2571; b) A. Mudring, *Aust. J. Chem.* **2010**, *63*, 544–564.
- [17] C. Zhong, T. Sasaki, A. Jimbo-Kobayashi, E. Fujiwara, A. Kobayashi, M. Tada, Y. Iwasawa, *Bull. Chem. Soc. Jpn.* **2007**, *80*, 2365–2374.
- [18] R. S. Rowland, R. Taylor, *J. Phys. Chem.* **1996**, *100*, 7384–7391.
- [19] a) C. Roth, T. Peppel, K. Fumino, M. Kockerling, R. Ludwig, *Angew. Chem.* **2010**, *122*, 10419–10423; *Angew. Chem. Int. Ed.* **2010**, *49*, 10221–10224; b) A. Wulf, K. Fumino, R. Ludwig, *Angew. Chem.* **2010**, *122*, 459–463; *Angew. Chem. Int. Ed.* **2010**, *49*, 449–453.
- [20] E. Arunan, G. R. Desiraju, R. A. Klein, J. Sadlej, S. Scheiner, I. Alkorta, D. C. Clary, R. H. Crabtree, J. J. Dannenberg, P. Hobza, H. G. Kjaergaard, A. C. Legon, B. Mennucci, D. J. Nesbitt, *Pure Appl. Chem.* **2011**, *83*, 1637–1641.
- [21] K. Fumino, A. Wulf, R. Ludwig, *Angew. Chem.* **2008**, *120*, 8859–8862; *Angew. Chem. Int. Ed.* **2008**, *47*, 8731–8734.
- [22] I. Skarmoutsos, D. Dellis, R. P. Matthews, T. Welton, P. A. Hunt, *J. Phys. Chem. B* **2012**, *116*, 4921–4933.
- [23] K. Matsumoto, R. Hagiwara, Z. Mazej, P. Benkić, B. Žemva, *Solid State Sci.* **2006**, *8*, 1250–1257.
- [24] a) K. Fumino, T. Peppel, M. Geppert-Rybczynska, D. H. Zaitsev, J. K. Lehmann, S. P. Verevkin, M. Kockerling, R. Ludwig, *Phys. Chem. Chem. Phys.* **2011**, *13*, 14064–14075; b) T. Peppel, C. Roth, K. Fumino, D. Paschek, M. Kockerling, R. Ludwig, *Angew. Chem.* **2011**, *123*, 6791–6795; *Angew. Chem. Int. Ed.* **2011**, *50*, 6661–6665.
- [25] I. de Pedro, A. García Saiz, J. A. Gonzalez, I. Ruiz de Larramendi, T. Rojo, C. Afonso, S. Simeonov, J. C. Waerenborgh, J. A. Blanco, J. Rogriguez, *Phys. Chem. Chem. Phys.* **2013**, *15*, 12724–12733.
- [26] J. C. Bonner, M. E. Fisher, *Phys. Rev.* **1964**, *135*, A640–A658.
- [27] G. S. Rushbrooke, P. J. Wood, *Mol. Phys.* **1958**, *1*, 257–283.
- [28] a) J. A. Zora, K. R. Seddon, P. B. Hitchcock, C. B. Lowe, D. P. Shum, R. L. Carlin, *Inorg. Chem.* **1990**, *29*, 3302–3308; b) J. Campo, J. Luzón, F. Palacio, G. J. McIntyre, A. Millán, A. R. Wildes, *Phys. Rev. B* **2008**, *78*, 054415.
- [29] a) O. A. Petrenko, C. Ritter, M. Yethiraj, D. McK Paul, *Phys. Rev. Lett.* **1998**, *80*, 4570–4573; b) J. E. Greedan, C. R. Wiebe, A. S. Wills, J. R. Stewart, *Phys. Rev. B* **2002**, *65*, 184424.
- [30] A. Zheludev, A. Grand, E. Ressouche, J. Schweizer, B. G. Morin, A. J. Epstein, D. A. Dixon, J. S. Miller, *Angew. Chem.* **1994**, *106*, 1454–1457; *Angew. Chem. Int. Ed. Engl.* **1994**, *33*, 1397–1399.
- [31] B. N. Figgis, P. A. Reynolds, R. Mason, *Inorg. Chem.* **1984**, *23*, 1149–1153.

- [32] G. Román-Pérez, J. M. Soler, *Phys. Rev. Lett.* **2009**, *103*, 096102.
- [33] J. Kohanoff, C. Pinilla, T. G. Youngs, E. Artacho, J. M. Soler, *J. Chem. Phys.* **2011**, *135*, 154505.
- [34] a) C.-R. Lee, C.-C. Wang, K.-C. Chen, G.-H. Lee, Y. Wang, *J. Phys. Chem. A* **1999**, *103*, 156–165; b) B. N. Figgis, L. Khor, E. S. Kucharski, P. A. Reynolds, *Acta Crystallogr. Sect. B* **1992**, *48*, 144–151.
- [35] R. Caballol, O. Castell, F. Illas, I. de P. R. Moreira, J. P. Malrieu, *J. Phys. Chem. A* **1997**, *101*, 7860–7866.
- [36] M. M. Turnbull, C. P. Landee, B. M. Wells, *Coord. Chem. Rev.* **2005**, *249*, 2567–2576.

Received: September 11, 2013

Published online on December 10, 2013
